

phys. stat. sol. (a) **135**, 133 (1993)

Subject classification: 64.75; 78.70; S10.15

*Institute of Solid State Physics, University of Latvia, Riga¹) (a) and
Institute of Physics, Latvian Academy of Science, Salaspils²) (b)*

EXAFS and XANES Studies of $\text{Co}_x\text{Mg}_{1-x}\text{O}$ Solid Solutions Using a Laboratory EXAFS Spectrometer

By

A. KUZMIN (a), N. MIRONOVA (b), J. PURANS (a), and A. SAZONOV (a)

Studies of the local electronic structure and the short-range order in solid solutions $\text{Co}_x\text{Mg}_{1-x}\text{O}$ with x varying from 0.02 to 1.00 are carried out on the CoK-edge X-ray absorption spectra using a laboratory EXAFS spectrometer. A non-monotonous change of the Co–O distance in the first coordination shell with a bent at about $x = 0.5$ is established. The second coordination shell of cobalt is formed by cobalt and magnesium atoms with a distribution close to a statistical one.

По К-краю рентгеновских спектров поглощения кобальта проведены исследования локальной электронной структуры и ближнего порядка в твердых растворах $\text{Co}_x\text{Mg}_{1-x}\text{O}$ в ряду от $x = 0,02$ до 1,00 на лабораторном EXAFS-спектрометре. Установлено немонотонное изменение расстояния Co–O в первой координационной сфере с перегибом около $x = 0,5$. Вторая координационная сфера кобальта образована атомами кобальта и магния с распределением близким к статистическому.

1. Introduction

The CoO–MgO binary system forms a continuous series of solid solutions and at any composition has a face-centered cubic lattice of the NaCl type, the parameter of which, according to X-ray diffraction data, depends linearly on the composition [1]. The radii of Co (0.079 nm) and Mg (0.071 nm) cations differ strongly, therefore during the formation of solid solutions a static homogeneous deformation of the crystalline lattice and statistical local deformation created by the substituting ion should be observed.

Studies of solid solutions by the EXAFS method allow to determine structural parameters in the short-range order of the absorbing atom, but XANES investigations give us information about its local electronic structure [2, 3].

The investigations of the $\text{Co}_x\text{Mg}_{1-x}\text{O}$ system at $x = 0.05$ by EXAFS and XANES methods have been reported earlier [4]. It is established that at this concentration the Co ions are statistically distributed in the MgO lattice.

The present paper deals with EXAFS studies of the short-range order of $\text{Co}_x\text{Mg}_{1-x}\text{O}$ solid solutions in the range from $x = 0.02$ to 1.00 on the CoK edge using the laboratory EXAFS spectrometer. A non-linear change of the Co–O distance in the first coordination shell with an inflection at $x = 0.5$ has been established. It was found that the second coordination shell of cobalt is formed by cobalt and magnesium ions with distribution close to a statistical one.

¹) Kengaraga 8, 226063 Riga, Latvia.

²) 229021 Salaspils, Latvia.

The local electronic structure has been investigated on the XANES spectra. The pre-edge part of the spectrum is very sensitive to the substitution of magnesium for cobalt that means that cations in the second and the following coordination shells practically do not give any contribution to the p-character of excited states (the bottom and the middle parts of the conduction band). Above the absorption edge (the upper part of the conduction band) their substitution influences essentially the shape of the absorption spectrum.

2. Experiment and Sample Preparation

Solid solutions $\text{Co}_x\text{Mg}_{1-x}\text{O}$ with $x = 0.02, 0.05, 0.10, 0.20, 0.50, 0.90, 1.00$ have been obtained using ceramics technology by a solid phase reaction method as a result of decomposition of oxygen-containing salts of magnesium and cobalt ($\text{MeSO}_4, \text{MeCO}_3$) at 1200°C . The annealing of the polycrystalline components was carried out at 970°C in air and then quickly cooled down to room temperature. Besides, pure CoO before measuring was annealed in vacuum at 400°C to provide the necessary stoichiometry of the sample.

X-ray structural and phase analyses were carried out to control the prepared samples. The composition of the solid solutions was established by instrumental neutron-activated analysis. It is found that the obtained solid solutions are single phase and the parameter of the face-centered cubic crystalline lattice changes linearly in the whole range of compositions in accordance with [1].

The X-ray absorption spectra of the cobalt K-edge were measured in transmission mode using the laboratory EXAFS spectrometer made in the Institute of Solid State Physics (Riga) [5]. To focus the X-ray radiation, the Johann scheme with bent α -quartz ($10\bar{1}1$) crystal monochromator was used. During measurements the bend of the crystal remained constant. In this case the defocusing of radiation was insignificant (the change of intensity up to 600 eV above the absorption edge did not exceed 10%). The counting rate of the monochromatized zero beam from the molybdenum tube, operated at 28 kV and 30 mA, was 10^5 counts/s with the resolution 6 eV.

The absorption coefficient $\mu(E)$ was determined in accordance with results of a subsequent measurement of the X-ray radiation intensity without the sample (I_0) and with the sample (I) during two passages over to whole energy range. Measurements were carried out on polycrystalline samples of 5 to 20 μm thickness deposited on an organic substrate.

The extraction of the EXAFS components from the absorption spectra was done by the standard procedure [6]. In the single scattering approximation the dependence of EXAFS oscillations $\chi(k)$ on the wave vector k has the following form:

$$\chi(k) = \sum_i \frac{N_i S_{0i}^2}{k R_i^2} f_i(\pi, k) e^{-2\sigma_i^2 k^2} e^{-2R_i/\lambda(k)} \sin\left(2kR_i + \varphi_i(\pi, k) + \frac{2R_i \Delta E_{0i}}{7.62k}\right), \quad (1)$$

where N_i is the coordination number of the i -shell, R_i the radius of the i -shell, σ_i the Debye-Waller factor, S_{0i}^2 the scale factor taking into account the influence of multielectron effects, $\lambda(k)$ is the mean free path of the photoelectron, $f(\pi, k)$ the backscattering amplitude of the photoelectron by atoms of the i -coordination shell, $\varphi(\pi, k)$ the phase shift determined by central and scattering atoms, and ΔE_{0i} the correction of absorption edge position and phase shifts.

The values of amplitude and phase shift calculated in the spherical wave approximation were taken from [7, 8]. The mean free path was approximated by the formula $\lambda(k) = k/\Gamma$,

where Γ is the width of the state, which depends on the width of the initial and final states, experimental resolution, and interaction of the photoelectron with the medium and nearest surroundings.

3. Results and Discussion

3.1 EXAFS

Experimental EXAFS spectra $\chi(k) k^2$ are shown in Fig. 1. The energy origin E_0 was selected in the edge region at the first derivative maximum of the absorption coefficient $\mu(E)$. The high frequency noise component was taken away by Fourier filtration of the signal in the interval from 0 to 0.7 nm. As is seen from Fig. 1, the experimental spectra are recorded using the laboratory spectrometer with a sufficient accuracy and reproduction at concentrations up to several per cent of cobalt in the MgO matrix. The FTs (see Fig. 2) of the experimental spectra were calculated with a rectangular window in the interval of wave vectors from 10 to 110 nm^{-1} . The identification of separate peaks is shown for pure CoO up to the seventh coordination shell in the single scattering approximation.

A detailed analysis of the first coordination shell parameters: the distances Co–O (R_1), the values of Debye-Waller factors (σ_1), and the coordination numbers (N_1), was realized by fitting the EXAFS signal obtained by the FT filtering in the interval from 0.07 to 0.2 nm. The best agreement with the crystallographic data for pure CoO [9] we obtained with theoretical phases and amplitudes calculated in the spherical wave approximation in [8]. Besides, the use of phases and amplitudes in the spherical wave approximation allowed us to fit our spectra from smaller values of wave vectors: from 10 to 110 nm^{-1} . For pure CoO the product NS_0^2 amounted to 2.8 ± 0.2 corresponding to the value S_0^2 equal to 0.46. A

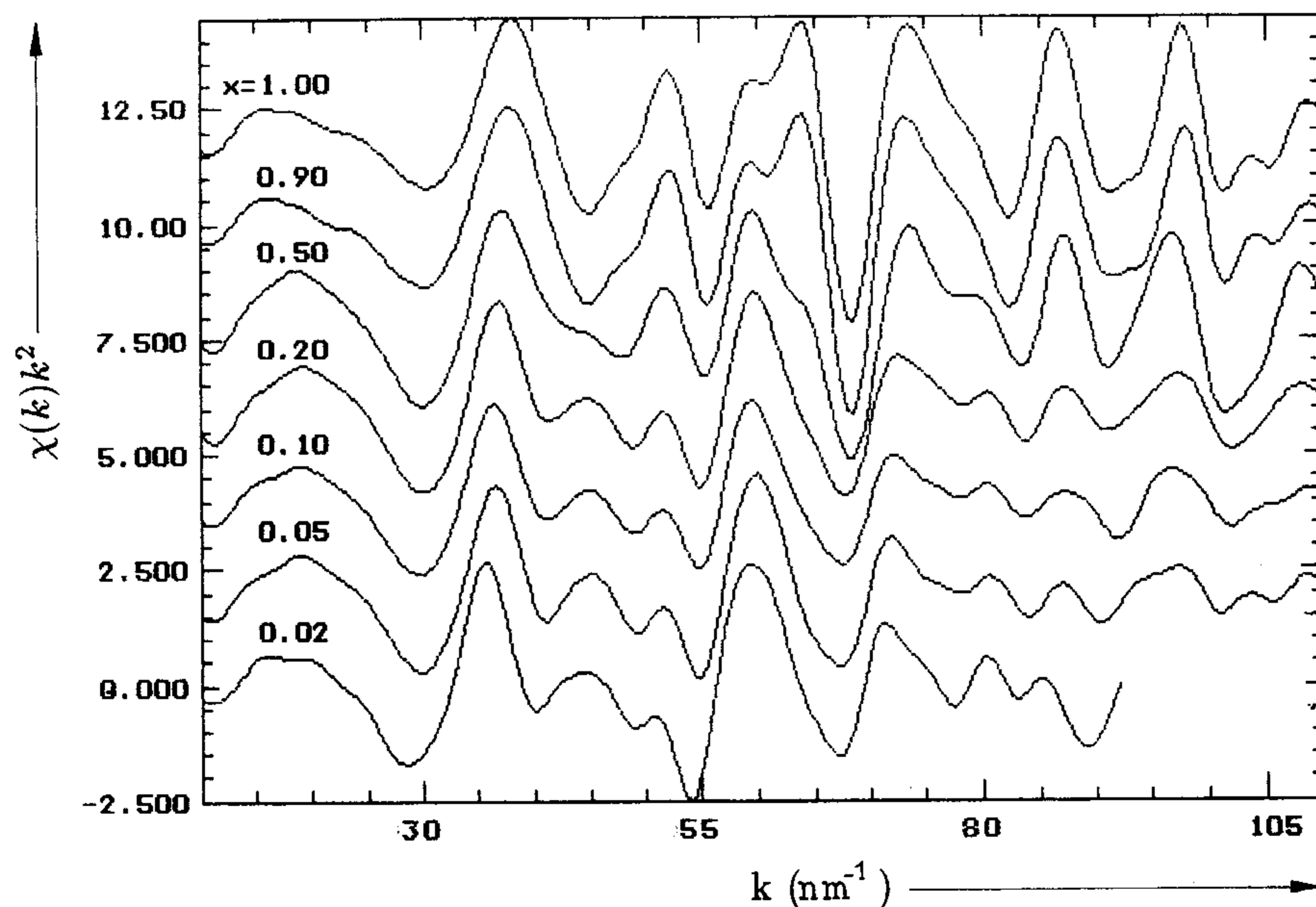


Fig. 1. Experimental EXAFS spectra $\chi(k) k^2$ of $\text{Co}_x\text{Mg}_{1-x}\text{O}$ solid solutions

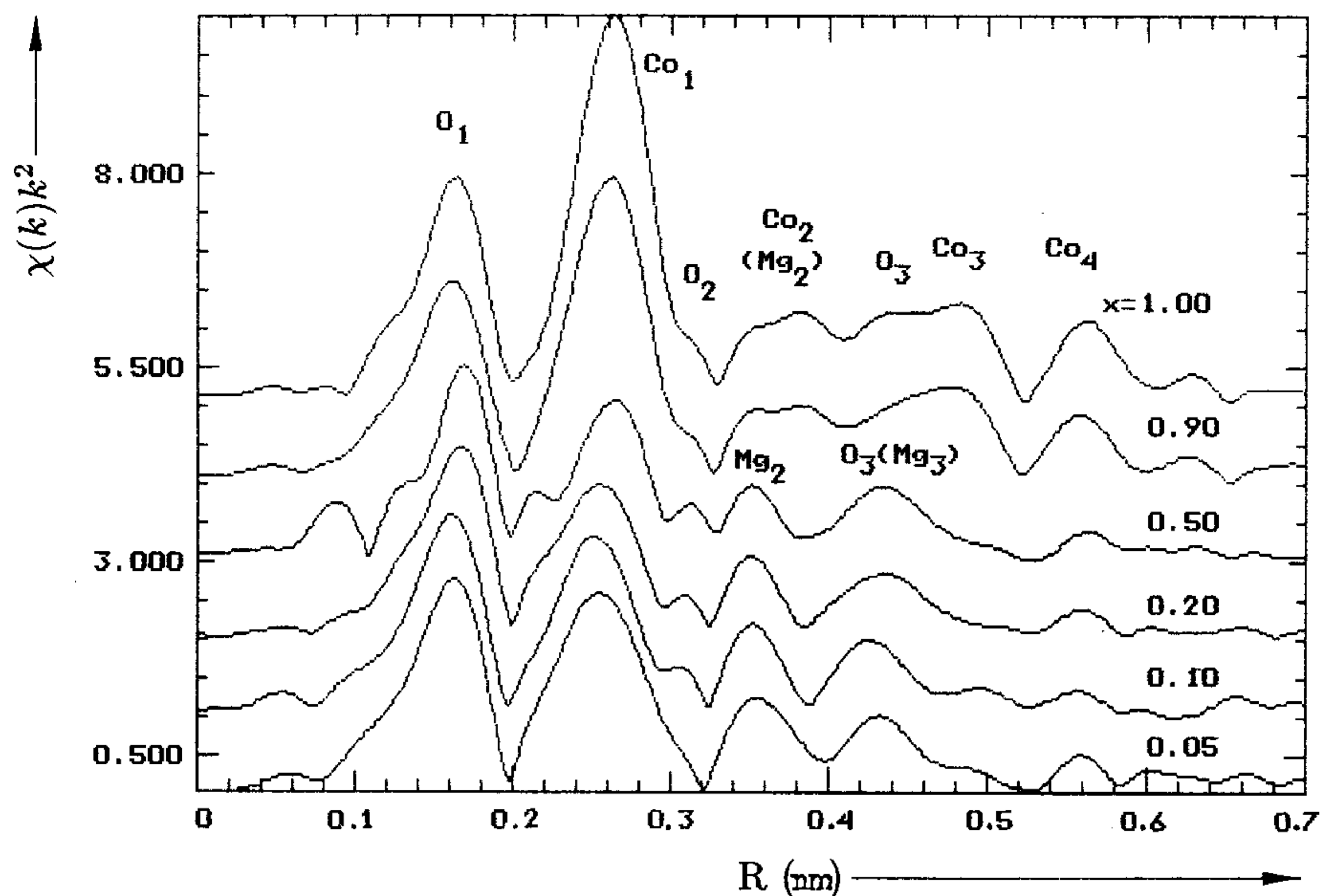


Fig. 2. Fourier transforms of EXAFS spectra $\chi(k) k^2$ shown in Fig. 1. The first seven coordination shells are marked

little lower value of the latter factor in comparison with the one in spectra taken with a high resolution at the synchrotron is explained by the lower resolution of the laboratory spectrometer. The Debye-Waller factor for the whole range of solid solutions within the error of the experiment did not change and was equal to $\sigma_1^2 = (0.005 \pm 0.001) \times 10^{-2} \text{ nm}^2$. From this we conclude that it is mainly determined by thermal vibrations, but the local deformations connected with the difference of the ion radii of cobalt and magnesium give a comparatively small contribution to the value of the Debye-Waller factor. The constant Γ , characterizing the natural width of the line and the experimental resolution, changed from 30 to 32 nm^{-2} in the range of the solutions and was mainly determined by the spectral resolution of the spectrometer. The most essential changes in the solid solutions are observed from distances Co–O in the first coordination shell. In Fig. 3 the dependence of the Co–O distance on the composition is shown. The accuracy of its determination is about $\pm 0.0005 \text{ nm}$. It was checked by repeated experiments and the analysis of fitting parameters which also includes the error in the choice of E_0 and the error of the fitting procedure. An analogous dependence of the distance change was obtained from the comparison of experimental phase spectra. At high concentrations of cobalt up to $x = 0.5$ the distance Co–O practically does not change and thereafter decreases to 0.002 nm. As is seen in Fig. 3, the non-monotonous curve with a bend in the region $x = 0.5$ essentially exceeds the experimental errors.

The second peak Co–Co (Mg) in Fig. 2 corresponds to twelve atoms of Co (Mg) in the second coordination shell of cobalt. EXAFS signals from the second coordination shell were obtained by the back FT procedure in the interval from 0.20 to 0.32 nm. The fit of parameters for pure CoO gives the following values. $R_2 = (0.3015 \pm 0.0005) \text{ nm}$, $\sigma_2^2 = (0.0075 \pm 0.005) \times 10^{-2} \text{ nm}^2$, $S_0^2 = 0.7 \pm 0.1$, $\Gamma = 50 \text{ nm}^{-2}$. The distance Co–Co well agrees with

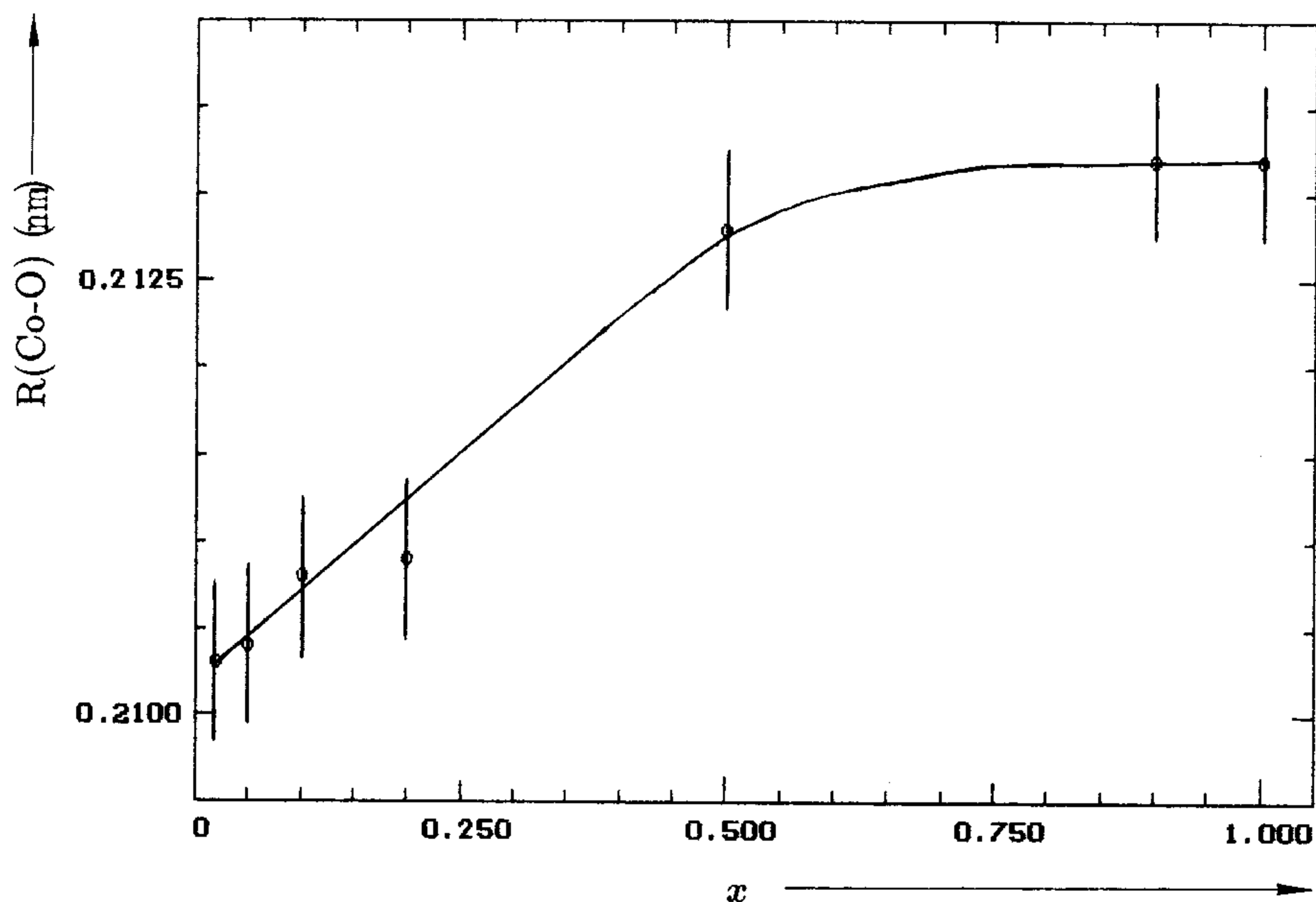


Fig. 3. The dependence of the Co–O distance in the first coordination shell from the concentration of cobalt ions in solid solutions $\text{Co}_x\text{Mg}_{1-x}\text{O}$

crystallographic data $R = 0.3012$ nm [9]. With the decrease of the cobalt concentration in a solid solution an essential decrease of the peak amplitude in the FT is observed, but at low concentrations a certain growth of its amplitude is observed. It should be noted that the amplitude of the first peak (Co–O) does not change within the error of the experiment. Besides, the effect is accompanied by the shift of the peak to smaller distances. A detailed analysis of the EXAFS signal from the second coordination shell of cobalt proved that the effect is connected with the interference of the backscattering signals from cobalt and magnesium atoms statistically distributed there. The cobalt and magnesium atoms differ essentially in the amplitude and phase of the photoelectron backscattering [7] that is displayed in Fig. 4 as the displacement of the modulus maximum of the EXAFS signal amplitude to smaller wave vectors (from 80 nm^{-1} at $x = 10.0$ to 55 nm^{-1} at $x = 0.05$) and in the displacement of the positions of maxima and minima of the signal (the phase changes almost by 90°). The comparison of the data for Co–Co and Co–Mg pairs shows that the local change of the distance coincides with that expected from the crystallographic data for pure CoO and MgO, i.e. a decrease of the distance by 0.0015 nm. It is interesting to note the increase of the Debye-Waller factor value connected with the growth of the thermal vibration amplitude in accordance with the smaller mass of magnesium atoms in comparison with cobalt.

In Fig. 2 the change of the position and the shape of peaks is well observed in the third and the following coordination shells that is connected with the substitution of cobalt for magnesium. A further detailed modeling of these peaks and EXAFS signals taking into account the effects of multiple scattering can give more detailed information on the correlation in the distribution of atoms and the local deformations in chains of three and four atoms in a solid solution. Such an analysis is in progress and will be reported in a forthcoming publication.

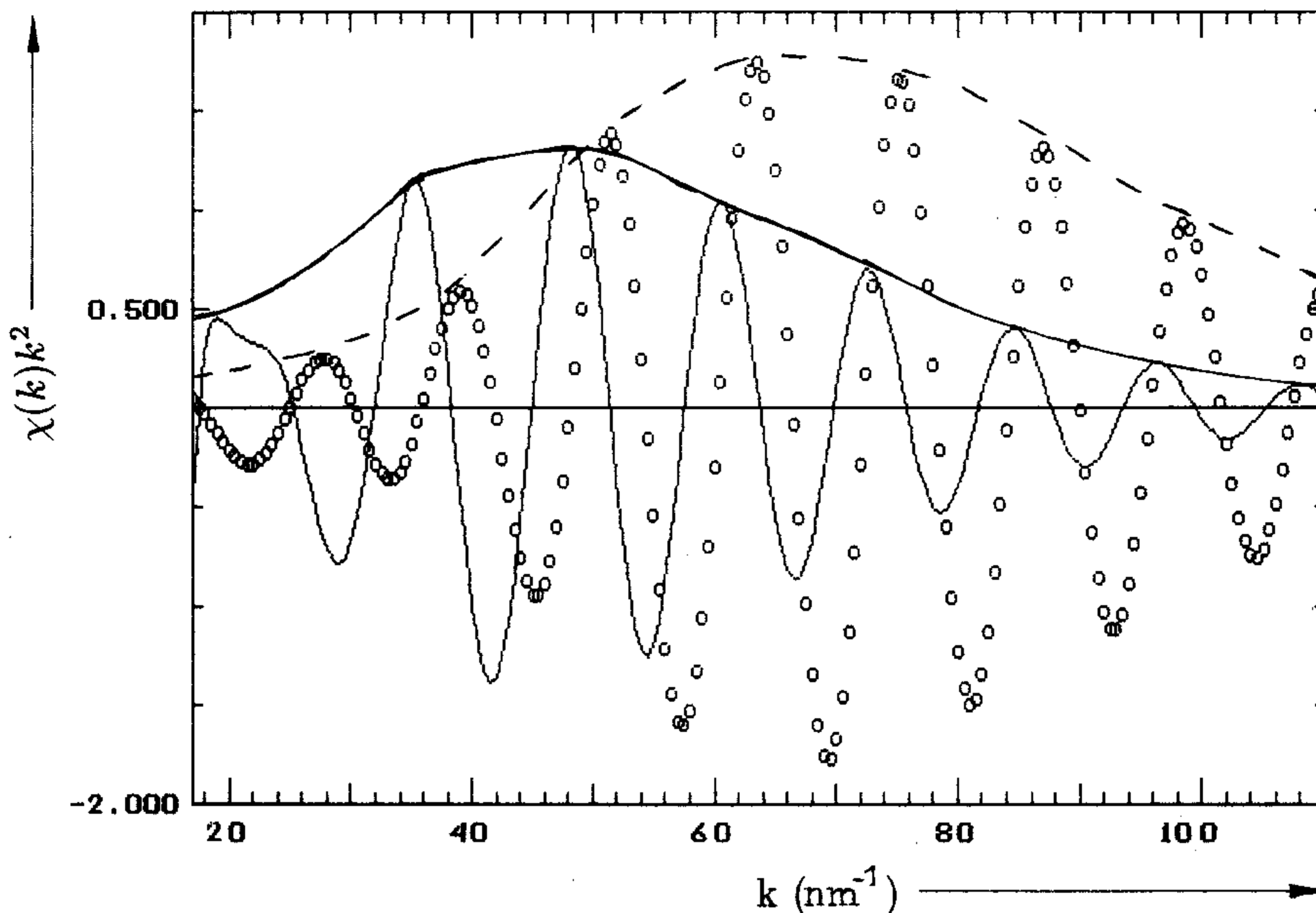


Fig. 4. Calculated EXAFS spectra $\chi(k)k^2$ for Co-Mg (solid line) and Co-Co (circles). One can see the difference between cobalt and magnesium backscattering amplitudes and phases

3.2 XANES

In Fig. 5 the XANES spectra and their first derivatives in the range of solid solutions $\text{Co}_x\text{Mg}_{1-x}\text{O}$ from $x = 0.02$ to 1.00 are shown. The position of maximum of the first derivative corresponds to the energy 7711 eV. In the region of the absorption edge it is possible to single out six features: A', A, B, C, D, E, which can be interpreted as the transitions of the photoelectron excited from the 1s(Co) level to bound states and processes of its scattering by the local surroundings.

The feature A', located before the main absorption edge corresponds to the transition $1s \rightarrow 3d(t_{2g} + e_g)[\text{Co}] + 2p[\text{O}]$. In the dipole approximation the transitions of the $ns \rightarrow md$ type in a regular octahedron are forbidden, therefore, the intensity A' is very weak and is due to the insignificant distortions of the octahedron of the first coordination shell of cobalt by thermal vibrations and the mixing of 2p states of oxygen.

The shoulder A located on the absorption edge in the atomic approximation corresponds to the forbidden transition $1s \rightarrow 4s$. Its high intensity is due to the mixing of 4s and 4p cobalt states, due to the oxygen atoms situated in the third coordination shell. The analogous effect was observed earlier [10] in compounds of with perovskite structure KMF_3 ($M = \text{Mn}, \text{Fe}, \text{Co}, \text{Ni}, \text{Cu}, \text{Zn}$), where it was found that the 4s state of potassium can mix the 4s and 4p states of metal M. In the formalism of multiple scattering of a photoelectron, the shoulder A corresponds to the resonance scattering of the wave with s-symmetry by the oxygen atoms (O_2) in the third coordination shell. In Fig. 6 the dependence of the amplitude of peak A on the concentration of cobalt ions is shown. During the formation of solid solutions a local deformation of the crystalline structure of MgO takes place produced by each

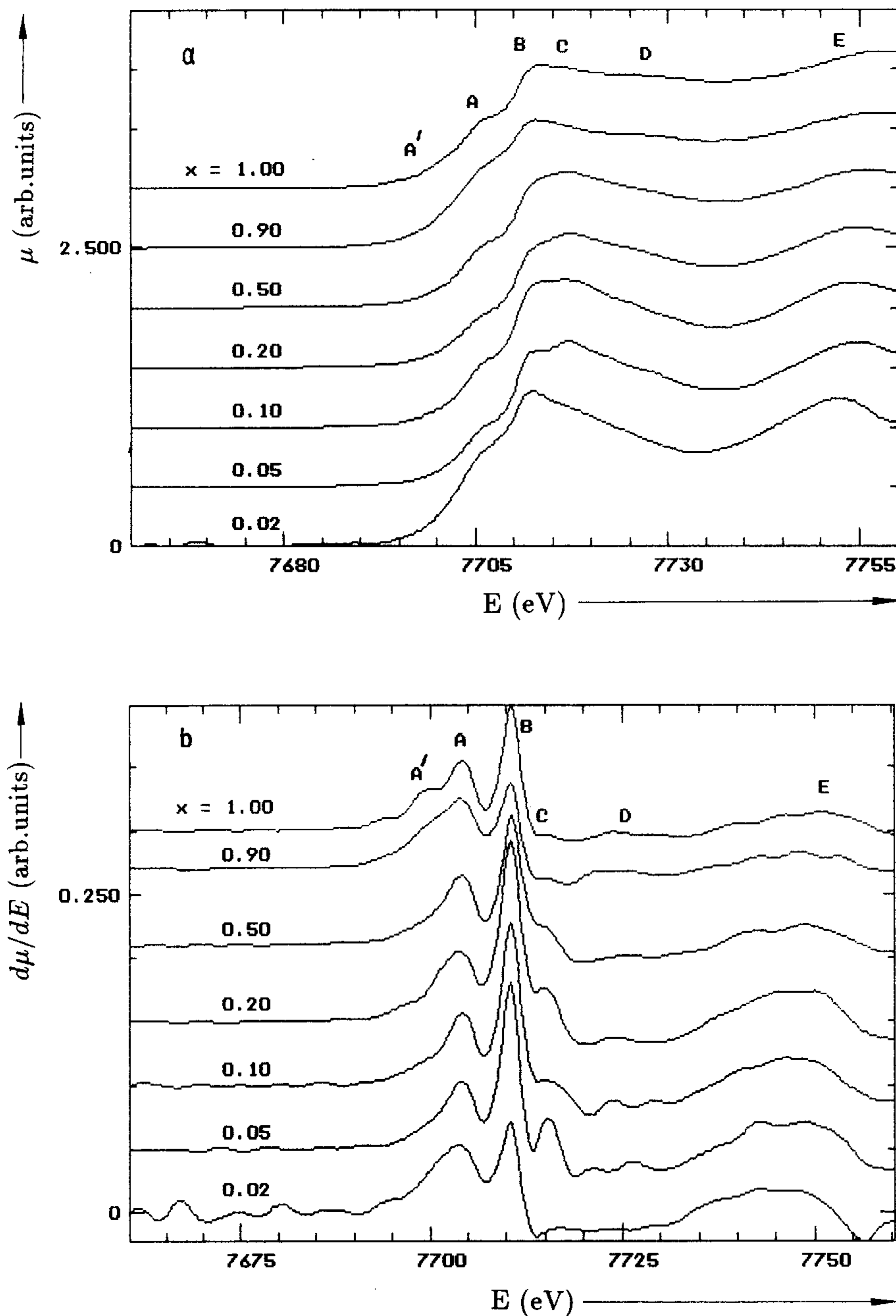


Fig. 5. a) XANES spectra of the CoK-edge and b) their first derivatives in solid solutions $\text{Co}_x\text{Mg}_{1-x}\text{O}$

substituting cobalt ion. The decrease of the distance $\text{Co}-\text{O}_2$ leads to a big mixing of 4s and 4p states of cobalt but the decrease of the local lattice distortion leads to the improvement of resonance conditions.

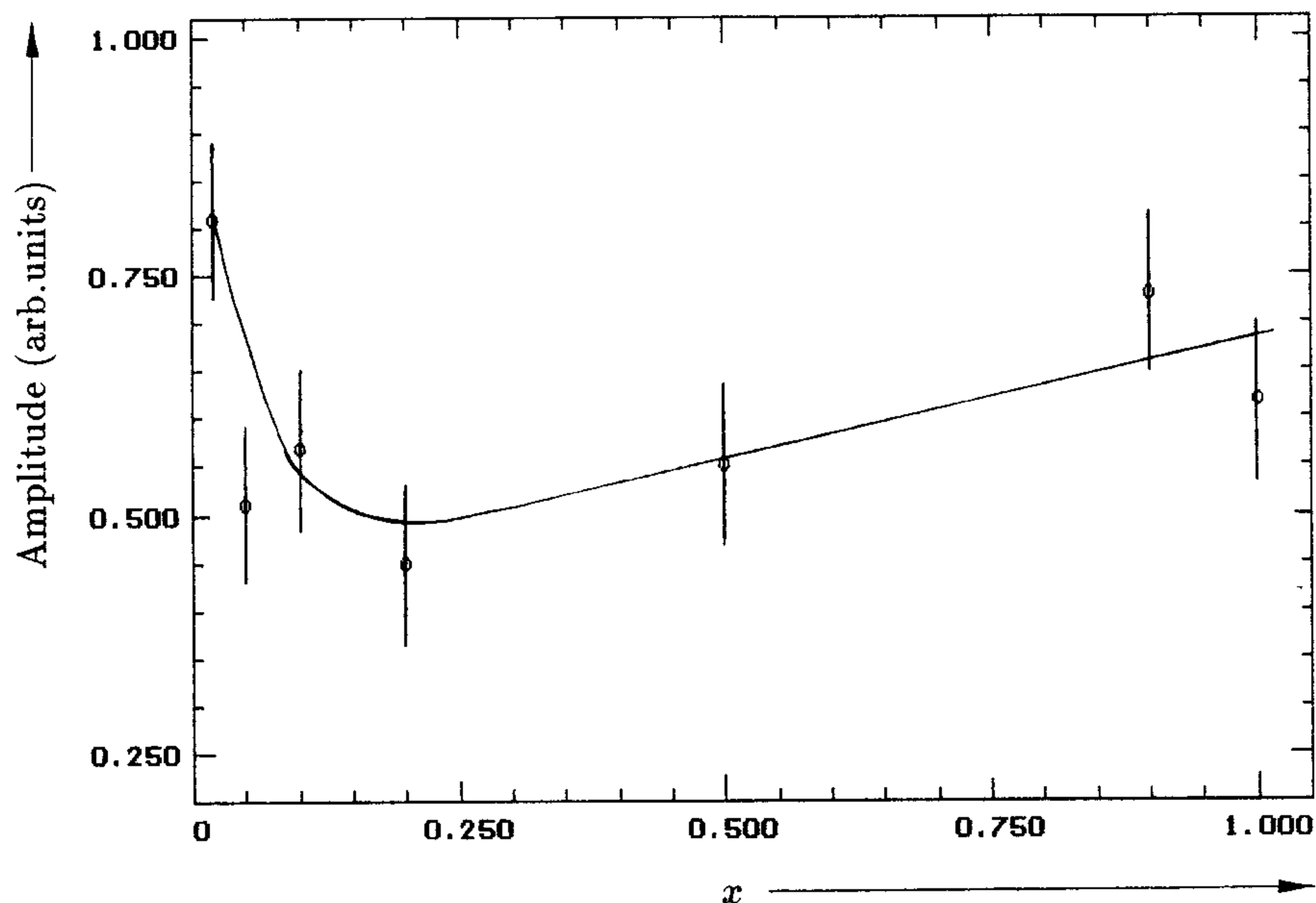


Fig. 6. The dependence of the amplitude of shoulder A on the concentration of cobalt ions in solid solutions $\text{Co}_x\text{Mg}_{1-x}\text{O}$

The main maximum B corresponds to the allowed transition $1s \rightarrow 4p[\text{Co}] + 2p[\text{O}]$. In the multiple scattering approach the peak B corresponds to the resonance scattering of the photoelectron by oxygens in the first coordination shell (O_1). The feature C corresponds to the transition $1s \rightarrow 5p$ into delocalized p states of the conduction band. The substitution of magnesium ions by cobalt ions leads to the statistical distribution of ions of both types in the cation sublattice and the decrease of the degree of delocalization of 5p states, leading to the increase of the amplitude of the C peak. The bend D corresponds to the resonance scattering of the photoelectron by oxygen atoms (O_2) in the third coordination shell (Fig. 7). Peak E corresponds to the resonance scattering of the photoelectron by oxygen atoms (O_1) in the first coordination shell.

4. Conclusions

The X-ray absorption spectra of the CoK-edge in $\text{Co}_x\text{Mg}_{1-x}\text{O}$ (with x from 0.02 to 1.00) solid solutions were studied using the laboratory EXAFS spectrometer. The analysis of both EXAFS and XANES parts of the experimental spectra is considered.

In the series of solid solutions $\text{Co}_x\text{Mg}_{1-x}\text{O}$ a statistical distribution of cobalt and magnesium atoms with insignificant local deformations is observed and does not exceed the amplitude of thermal vibrations at room temperature. In the first coordination shell of cobalt the distance Co–O decreases non-monotonously by 0.002 nm with a bend at $x = 0.5$ at the substitution of cobalt for magnesium. In the second coordination shell the interatomic distance in the Co–Co pair (in CoO) is on by 0.0015 nm larger than in the Co–Mg pair in the solid solution with $x = 0.05$. The substitution of cobalt cations for magnesium in the second and the following coordination shells of cobalt practically does not change the

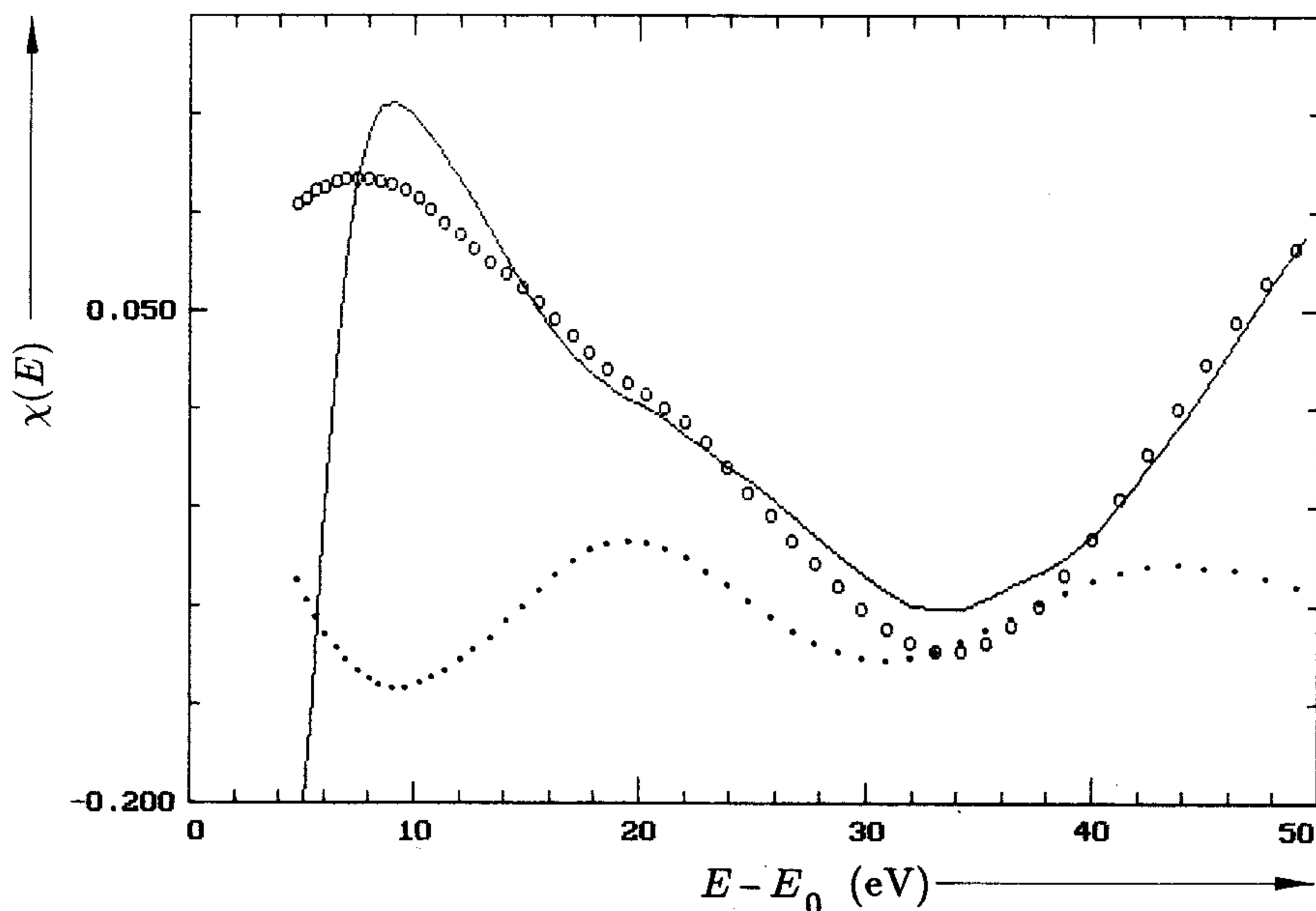


Fig. 7. XANES spectra of the CoK-edge in CoO. Solid line experiment, circles calculation in the single scattering approximation of the photoelectron by the atoms of the first, second, and third coordination shells, dotted curve contribution from the scattering by the oxygen atoms in the third shell

contribution to the p-character of excited states of cobalt in the pre-edge part of the XANES spectrum (the lower part and the bottom of the conduction band), but essentially influences the formation of states beyond the absorption edge (the upper part of the conduction band).

References

- [1] N. A. MIRONOVA and U. A. ULMANIS, Radiation Defects and Metal Ions of Iron Group in Oxides, Izd. Zinatne, Riga 1988 (in Russian).
- [2] P. A. LEE, P. H. CITRIN, P. EISENBERGER, and B. M. KINCAID, Rev. mod. Phys. **53**, 769 (1981).
- [3] J. WONG, Mater. Sci. Engng. **80**, 107 (1986).
- [4] K. ASAKURA and Y. IWASAWA, Mater. Chem. Phys. **18**, 499 (1988).
- [5] A. J. KUZMIN and A. I. SAZONOV, 6th Sci. Conf. Institute of Solid State Physics (Abstracts), Latvian University, Riga 1990 (p. 38) (in Russian).
- [6] B.-K. TEO, EXAFS: Basic Principles and Data Analysis, Springer-Verlag, Berlin 1986.
- [7] A. G. MCKALE, B. W. VEAL, A. P. PAULIKAS, S.-K. CHAN, and G. S. KNAPP, J. Amer. Chem. Soc. **110**, 3763 (1988).
- [8] A. G. MCKALE, G. S. KNAPP, and S.-K. CHAN, Phys. Rev. B **33**, 841 (1986).
- [9] L. I. MIRKIN, Handbook on X-Ray Structural Analysis of Polycrystals, Izd. Fizmatgiz, Moscow 1961 (in Russian).
- [10] M. KITAMURA and S. MURAMATSU, Phys. Rev. B **41**, 1158 (1990).

(Received April 1, 1992; in revised form October 26, 1992)